



REMOVAL OF Se(IV) AND Se(VI) FROM WATER BY ALUMINUM-OXIDE-COATED SAND

WEN-HUI KUAN¹*, SHANG-LIEN LO¹®, MING K. WANG² and
 CHENG-FANG LIN¹

¹Graduate Institute of Environmental Engineering and ²Department of Agricultural Chemistry,
 National Taiwan University, Taipei, 106, Taiwan, R.O.C.

(First received February 1997; accepted in revised form June 1997)

Abstract—Aluminum-oxide-coated sand (AOCS) was evaluated for the removal of selenite (Se(IV)) and selenate (Se(VI)) from water. Quartz sand was coated at 70°C using 1 M AlCl₃ solution aging for 2 d at various coating pH (pH_(coating)). The characteristics of the AOCS surface were pH_(coating)-dependent. The Al oxide coating was an X-ray noncrystalline, porous compound at low pH_(coating), while at high pH_(coating), the AOCS could better withstand acid/alkali and the coatings tended to form crystalline boehmite and bayerite. Adsorption of Se(IV) and Se(VI) was more effective using sand coated at low pH_(coating) than at high pH_(coating). AOCS produced at pH_(coating) 5.98 had optimum properties and was employed as the adsorbent for the present adsorption studies. Adsorption experiments of Se(IV) and Se(VI) by AOCS performed as a function of pH, initial concentration, reaction time, and competing ion concentrations were examined. Removal of Se(IV) and Se(VI) increased with decreasing pH but was obviously greater for Se(IV) than Se(VI). In Se(IV) and Se(VI) mixed systems, the adsorption of Se(IV) was evidently inhibited by Se(VI) only at system pH ranging from 3 to 8, and the degree of inhibition was similar at Se(VI) to Se(IV) molar ratios of 1 and 3. However, Se(VI) adsorption significantly decreased with increasing Se(IV) concentration at all system pH. The sequence of foreign anions competing with respect to Se(IV) and Se(VI) adsorption was in the order of SO₄²⁻ > HCO₃⁻. © 1998 Elsevier Science Ltd. All rights reserved

Key words—aluminum-oxide-coated sand, Se(IV), Se(VI), coating, adsorption

INTRODUCTION

Selenite (SeO₃²⁻) and selenate (SeO₄²⁻) are the dominant forms of selenium existing in aqueous systems (Jacobs, 1989). In accordance with its content, Se can either be essential or toxic to humans, animals, and certain plants (Lakin, 1973; Alloway, 1995). As water quality standards become stricter, conventional drinking water treatments such as coagulation, sedimentation, and filtration are constrained in removing trace amounts of heavy metals. Typically, Al and Fe salts extensively serve as coagulants in conventional treatment processes. Since the coagulated metal oxides/hydroxides are limited to reactor configurations incorporating large sedimentation basins or filtration units and add substantially to the cost of sludge disposal, the developed technique for coating metal oxides/hydroxides onto filter sand surfaces is applied to overcome some of these disadvantages in water treatment.

Aluminum and iron oxides are abundant in natural environments and both have relatively high surface area and variable surface charge. During the past decade, several researchers have developed an

innovative technique for coating Fe oxides onto sand surface to effectively remove/recover trace heavy metals (Edwards and Benjamin, 1989; Bailey *et al.*, 1992; Stahl and James, 1991; Lo *et al.*, 1994; Lai *et al.*, 1994). However, sand surface covered by Al hydrolysis products has not been evaluated for the removal of selenium to date.

For implication of metal-oxide-coated sand in substantive utilization, it is important to consider the adhesive strength between the metal-oxide coatings and quartz sand. Meng and Letterman (1993a,b; 1996) studied binary oxide systems and suggested that the interaction between aluminum hydrolysis products and SiO₂ was relatively strong, while discrete Fe(OH)₃ colloids were formed in the presence of SiO₂ suspensions. Furthermore, it has been found that the sustenance of SiO₂ was significantly enhanced by the presence of Al(OH)₃, aluminum-oxide-coated sand (AOCS) was therefore necessary to be evaluated for its adsorption efficiency.

The objective of this study was to determine the effect of Al oxide mineralogy, amounts of oxide coatings, and acid- and alkali-resistance on the removal of selenium from water. A series of batch adsorption experiments was conducted to further demonstrate the efficiency of Se(IV) and Se(VI)

*Author to whom all correspondence should be addressed
 [Fax: 001-886-2-3928821].

removal by AOCS. X-ray diffractometry and scanning electron microscopy determinations helped to elucidate the apparent characteristics of AOCS surface. Acid- and alkali-resistance, which are the major factors influencing the working life of filter media in the regeneration process, were investigated to estimate AOCS stability. Moreover, competition adsorption of selenium in Se(IV)/Se(VI) mixed systems and with the co-existence of sulfate (SO_4^{2-}) or bicarbonate (HCO_3^-) was also examined to obtain a preliminary assessment for the removal efficiencies of Se(IV) and Se(VI) by AOCS in natural aqueous systems.

MATERIALS AND METHODS

AOCS preparation

Quartz sand was selected from # 20 ~ 25 mesh sieve (0.84 ~ 0.71 mm), soaked in 0.1 M HCl solution for 24 h, rinsed with de-ionized water, and then oven-dried at 105°C. The BET surface area of the pretreated sand was 0.20 m²/g. Al(III) stock solution of 1 M was prepared by dissolving $\text{AlCl}_3 \cdot 6\text{H}_2\text{O}$ in Milli-Q water. To make the Al oxide floc suspension, 4.0 M NaOH was added dropwise to 100 mL of stock solution to a desired pH, and the solution was mixed for about 15 mins. The suspension and 200 g sand were poured into a 1-L Pyrex glass beaker, and the mixture was oven-dried at 70°C for 2 d, during which time it was continuously stirred by a Teflon mixer. The AOCS was washed with de-ionized water until run-off was clear, redried at 70°C for 1 d, and finally stored in capped polystyrene bottles.

Characterization of AOCS

The oxide prepared by the above method without quartz sand was characterized by X-ray diffraction (XRD). The oriented samples were examined with an X-ray diffractometer (Rigaku Miniflex) using $\text{CuK}\alpha$ radiation generated at 30 kV and 10 mA. Total coated Al on the sand surface was determined by dissolving 5 g of AOCS in 50 mL of 6 M HCl for 24 h. Experiments for measuring acid- and alkali-resistance were conducted by soaking 5 g AOCS in HCl (pH = 3.0, 50 mL) and NaOH (pH = 12.0, 50 mL) for 24 h, respectively. The suspension was vacuum-filtered through a 0.2 μm membrane filter, and the Al content in the filtrate was determined using atomic absorption spectrophotometry (Perkin-Elmer 5000). Topography of the quartz sand and AOCS was examined by scanning electron microscopy (SEM). Samples were fixed onto aluminum stubs with double-stick tape, coated with gold, and viewed with JEOL JSM-t100 SEM.

Se adsorption experiments

For adsorption isotherm study, 50 mL of Se solution with 0.1 M NaCl for ionic strength was added to an Erlenmeyer flask along with 5 g AOCS produced at $\text{pH}_{(\text{coating})}$ 5.98. The suspension was shaken at 100 rpm for 3 h for batch experiments. The pH of the suspension was maintained within the desired range with dilute HCl and NaOH solutions during the entire adsorption process. Except for the adsorption and desorption kinetic tests, the reaction time of all other adsorption experiments was 3 h. After completion of reaction, the suspension was passed through a membrane filter (Millipore filter, 0.20 μm) and the filtrate was preserved at 4°C. Then, Se was analyzed by ion chromatography (IC, Dionex, model 2000i/sp) (Blaylock and James, 1993).

I Adsorption and desorption kinetics. For adsorption kinetic experiments, the initial concentration of either Se(IV) or Se(VI) was 0.8 mM. The suspension was shaken and pH was maintained at 4.80. Samples were taken at various times during an 8-hr period. Se-desorption kinetic experiments were performed after equilibrium experiments using an initial concentration of 1.2 mM Se(IV) at pH 4.00 or 1.0 mM Se(VI) at pH 4.80. The supernatant was discarded and 100 mL of NaOH solution (pH = 12) was added to the adsorbent remaining in the vessels. After each specified reaction time, the supernatant solution was separated from the sample by membrane filtration and the Se concentration was determined.

II Equilibrium adsorption. For pH adsorption-edge, the initial concentration of Se(IV) was set to 0.8, 1.2, 1.6, or 1.8 mM and of Se(VI) was 0.8, 1, or 1.2 mM. The suspension pH was maintained within the range of 3 ~ 12. Adsorption isotherms were studied by pouring 50 mL of 0 ~ 2 mM Se solution into an Erlenmeyer flask containing 5 g of AOCS at different solution pH values (4.90 ~ 8.40).

III Competition adsorption. Se(IV) and Se(VI) were mixed in the system (pH 3 ~ 12), and then adsorption experiments were conducted under the following conditions: (1) 1.2 mM Se(IV), Se(VI) to Se(IV) molar ratio = 0, 1, and 3; and (2) 0.8 mM Se(VI), Se(IV) to Se(VI) molar ratio = 0, 1, and 3. Experiments were also performed under an initial concentration of 1.2 mM Se(IV) at pH 7.80 or 0.8 Se(VI) at pH 6.80, with the concentration of foreign competing anions, SO_4^{2-} (Na_2SO_4) or HCO_3^- (NaHCO_3), ranging from 0 to 1.5 mM.

RESULTS AND DISCUSSION

Characterization of AOCS

The characteristics of AOCS formed under various coating conditions are summarized in Table 1. The pH value at which the aluminum oxides coat (2.00 ~ 12.50) is termed as $\text{pH}_{(\text{coating})}$. X-ray diffractograms of Al oxides (Fig. 1) showed an X-ray non-crystalline material under acidic coating condition and peaks (3.16, 2.35, 1.86, 1.85 and 1.77 Å) of boehmite (JCPDS 21-1307) formed at $\text{pH}_{(\text{coating})}$ ranging from 8.30 to 12.50. Additionally, Al oxides which precipitated at $\text{pH}_{(\text{coating})}$ higher than 10.77 also displayed intense 4.71, 4.35, 3.20, 2.46, 2.36, 2.22, 2.16, 2.07, 2.03, 1.98, 1.72 and 1.69 Å peaks of bayerite (JCPDS 20-11). These results indicated that increasing $\text{pH}_{(\text{coating})}$ causes the crystallinity of Al oxides to increase. The structure of boehmite (γ - AlOOH) is composed of double layers of oxygen and hydroxide in cubic packing. The double layers are joined by hydrogen bonds, and crystal exhibits preferential cleavage in the direction perpendicular to the direction of the hydrogen bonding. DeBoer *et al.* (1963) have determined the hydroxyl group density on boehmite surfaces to be 16.5 groups per nanometer square. Bayerite has the composition $\text{Al}(\text{OH})_3$ and grows preferentially in the way the double layers of coordinated hydroxyl and aluminum ions are stacked to form the three-dimensional crystal units. Therefore, a fraction of the bayerite surface is shielded by each layer and remains the edges of individual layers. Hence, the distribution of charge sites per unit area of bayerite would be

Table 1. Characteristics of AOCS formed at various pH_(coating)

pH _(coating)	2.00	3.60	4.80	5.98	7.18	8.30	9.30	10.77	11.50	12.50
Total amount of coated aluminum (mg Al/g sand)	2.30	1.48	2.78	3.73	1.45	1.47	1.80	3.32	3.75	4.00
Acid-resistance at pH 3 (dissolved Al/total Al × 100%)	3.83	3.68	3.98	1.91	13.91	10.48	3.93	0.15	0.53	0.53
Alkali-resistance at pH 12 (dissolved Al/total Al × 100%)	14.92	11.71	6.43	2.81	72.85	58.06	32.72	2.76	2.10	1.00
Crystallinity of aluminum oxides	—	—	—	—	—	—	+	++	+++	++++

^a + symbol indicates the degree of crystallinity of Al oxides, with increasing numbers of + representing higher degrees of crystallinity.

expected to be more sporadic than that of boehmite.

The adsorptive properties of the oxide surfaces in this study can be further related to their point of zero charge (pH_{pzc}). The pH_{pzc} has been determined as ranging from 7.5 ~ 9.5 for bayerite (Parks, 1965) and 10.4 for boehmite (Bleam and McBride, 1985). The increase in pH_{pzc} is attributed to localized strong positive charges on the boehmite surface as compared to the more diffuse distribution of surface charge sites on bayerite. Moreover, the adsorption capacities of AOCS surfaces may also vary with the degree of crystallinity of Al oxide coating, which affects the surface area, concentration of structural defects, and solubility product for aluminum hydroxides and oxyhydroxides. From the results shown in Table 1, it is readily seen that the AOCS was coated with less Al oxides at lower pH_(coating) conditions except pH_(coating) 5.98. Because the crystalline Al oxides are more apt to coat onto quartz sand than X-ray noncrystalline Al oxides are, the maximum of Al oxide coating occurred at pH_(coating) 12.50. Acid and alkali-resistance revealed that the amount of aluminum in an acidic or alkaline medium dissolved from crystalline Al oxides produced at pH_(coating) 10.77 ~ 12.50 was less than that of X-ray noncrystalline Al oxides at low pH_(coating). This is in accordance with the theoretical solubility of hydrous aluminum oxides of various crystallinity in aqueous solutions (Mason, 1960). Thus, AOCS produced at lower pH_(coating) shows less capability of resisting acidity/alkalinity, and its regeneration is limited when a strongly acidic or alkaline regenerating solution is used.

SEM images of quartz sand are shown in Fig. 2(1a) and Fig. 2(1b). SEM micrographs of AOCS formed at pH_(coating) 5.98 are illustrated in Fig. 2(2). The roughness of the sand surface was conducive to Al oxide coatings. The AOCS surfaces were shown to have flat and chapped-like morphology (see Fig. 2(2a)). Figure 2(2b) shows the SEM micrograph for the middle area of Fig. 2(2a) enlarged at 15,000 × magnification. It reveals that the chapped-like morphology is the result of Al oxides embedded in the hollows of the quartz sand surface. Figure 2(2c), magnification of the flat portion, shows that the surface is porous and completely differs from the Al oxide-free quartz sand, while the surface of AOCS formed at pH_(coating)

12.50 contains granules of bayerite which have crystallized well and accumulated significantly (Fig. 2(3)).

Table 2 demonstrates the effect of pH_(coating) on Se removal. The initial concentrations of Se(IV) and of Se(VI) were set to 1.6 mM and 0.8 mM, respectively, and the pH was maintained at 4.80 in each batch adsorption experiment. The adsorption efficiency was dependent on the formation of Al oxides. The Al oxides formed at pH_(coating) ≤ 9.30 were porous, X-ray noncrystalline, fine particles; hence, their adsorption of Se(IV) and Se(VI) was greater than that of AOCS produced at higher pH_(coating), even though the total amount of coated aluminum per unit weight of sand was less. The greatest adsorption of Se(IV) and Se(VI) onto AOCS occurred at pH_(coating) 5.98. The amount of coated Al was 3.73 mg Al/g sand when the AOCS was produced at pH_(coating) 5.98, and the amount of Al dissolved from coated Al oxides was 1.91% in acidic solution (pH = 3) and 2.81% in alkaline solution (pH = 12) (see Table 1). Therefore, AOCS prepared at pH_(coating) 5.98 was selected as the adsorbent for the following batch adsorption experiments.

Adsorption and desorption kinetics

Adsorption kinetics of Se(IV) and Se(VI) are shown in Fig. 3. Uptake of both Se(IV) and Se(VI) was rapid, and a metastable equilibrium state was reached within 60 mins. As a consequence, 3 h was chosen as the reaction time required to reach pseudo-equilibrium in the present "equilibrium" adsorption experiments. By increasing the alkaline concentration (i.e. pH 12), which caused the hydroxylation of Al oxides on the AOCS surface, the adsorbed anions were released and the AOCS could then be regenerated. Se(IV) and Se(VI) desorption kinetics shown in Fig. 4 reveal that approximately 3 h was needed for Se(VI) desorption to reach a 91% pseudo-steady state, while it took 5 h for Se(IV) desorption to reach 82%. Since Se(IV) strongly bonded to the metal oxide surface via the formation of inner-sphere complexes, desorption of Se(IV) is less exhaustive than Se(VI) in the alkaline regeneration process (Balistrieri and Chao, 1987; Hayes, 1987; Neal *et al.*, 1987; Zhang and Sparks, 1990; Scott and Morgan, 1996).

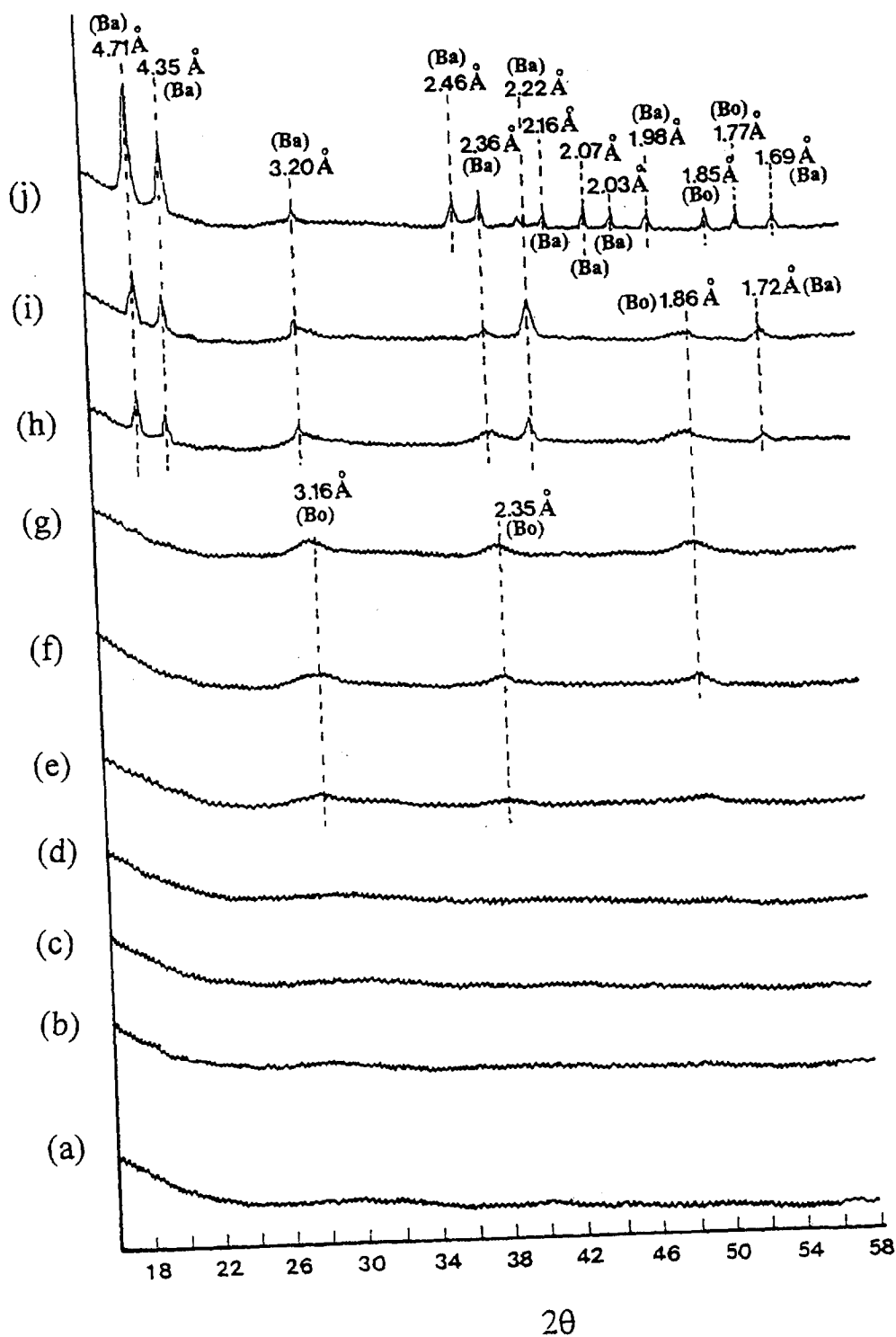


Fig. 1. X-ray diffractograms of Al oxides prepared at various $\text{pH}_{(\text{coating})}$: (a) 2.00; (b) 3.60; (c) 4.80; (d) 5.98; (e) 7.18; (f) 8.30; (g) 9.30; (h) 10.77; (i) 11.50; (j) 12.50 (Bo: boehmite; Ba: bayerite).

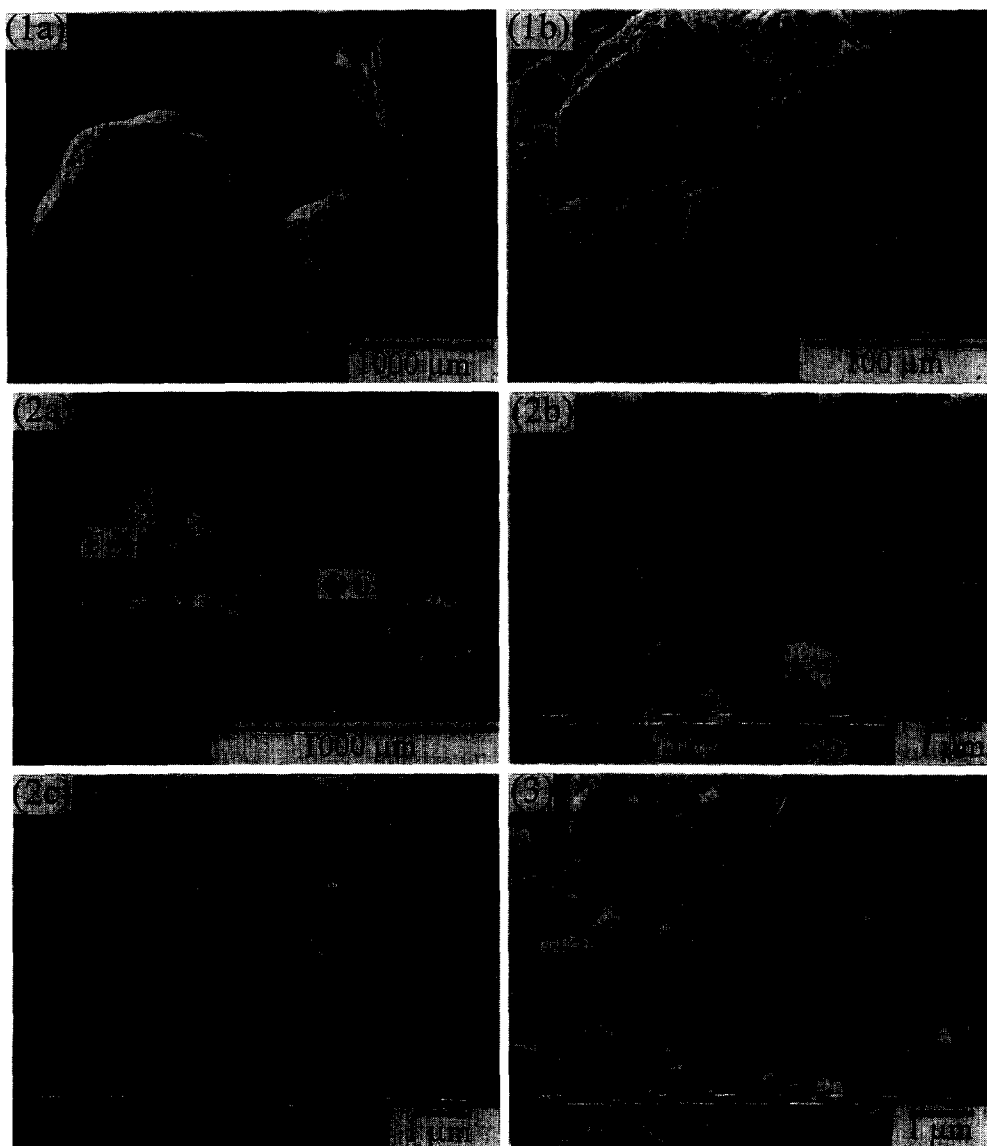
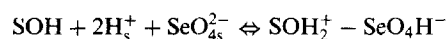


Fig. 2. SEM micrographs of (1) quartz sand; (2) AOCS formed at $\text{pH}_{(\text{coating})}$ 5.98 enlarged at various magnifications; and (3) AOCS formed at $\text{pH}_{(\text{coating})}$ 12.50 (F: flat; C: chapped-like portion).

Equilibrium adsorption

I pH-adsorption edge. For AOCS prepared at 70°C aging for 2 days using 1 M AlCl_3 solution at $\text{pH}_{(\text{coating})}$ 5.98, the amount of anions adsorbed by the AOCS surface is dependent upon the anionic characteristics and the type of adsorption site involved. In general, adsorption density depends upon the type of surface species formed. Previous surface complexation modeling studies (Davis and Leckie, 1980) describe that adsorbed Se(VI) is more easily protonated than those in bulk electrolyte solutions, and a qualitative predication for this phenomenon can be regarded as



where SOH represents an un-ionized surface site, and the subscript s denotes surface concentration.

Under the framework of surface complexation theory (Sposito, 1983; 1984; Dzombak and Morel, 1990), the standard Gibbs free energy of sorption ($\Delta G_{\text{sorp}}^\circ$) of Se(IV) or Se(VI) onto

Table 2. Removal of Se(IV) and Se(VI) by AOCS formed at various $\text{pH}_{(\text{coating})}$

$\text{pH}_{(\text{coating})}$	Se(IV) removed	Se(VI) removed
	(mg Se/g AOCS)	
2.00	0.79	0.60
3.60	0.64	0.33
4.80	0.66	0.37
5.98	1.05	0.63
7.18	0.56	0.23
8.30	0.56	0.22
9.30	0.58	0.23
10.77	0.62	0.26
11.50	0.61	0.24
12.50	0.56	0.21

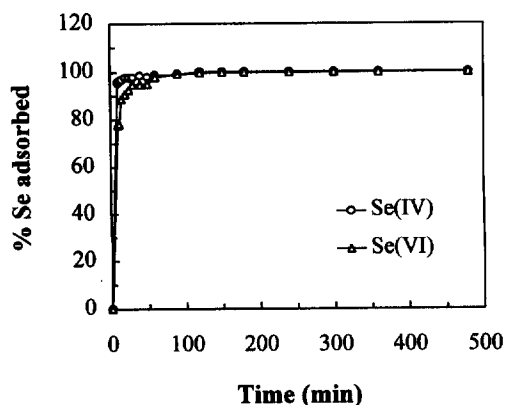


Fig. 3. Adsorption kinetics of Se(IV) and Se(VI) on AOCS (initial concentration of Se = 0.8 mM, pH = 4.80).

AOCS surfaces can be divided into two components according to

$$\Delta G_{\text{sorp}}^{\circ} = \Delta G_{\text{Coul}}^{\circ} + \Delta G_{\text{intr}}^{\circ}$$

where $\Delta G_{\text{Coul}}^{\circ}$ is the Coulombic term, which represents the contribution to the overall free energy of adsorption from interaction between the AOCS surface charge and the anion (Se(IV) or Se(VI)). The remaining free energy term $\Delta G_{\text{intr}}^{\circ}$ is thought to represent an intrinsic contribution characteristics of both the solid and the ion. It has been intensively pointed out that the value of $\Delta G_{\text{Coul}}^{\circ}$ is favorable for adsorption at low pH and unfavorable at high pH as the hydrous oxide bears a negative charge (Sposito, 1983; 1984; Dzombak and Morel, 1990).

The pH-adsorption edges of various concentrations of Se(IV) and Se(VI) are displayed in Fig. 5 and Fig. 6, respectively. When the initial concentration of Se(IV) increased, the adsorption edge curves shifted to the left because the number of adsorption sites remained fixed. If AOCS provides a sufficient number of adsorption sites, Se(IV) adsorption density will increase with higher surface

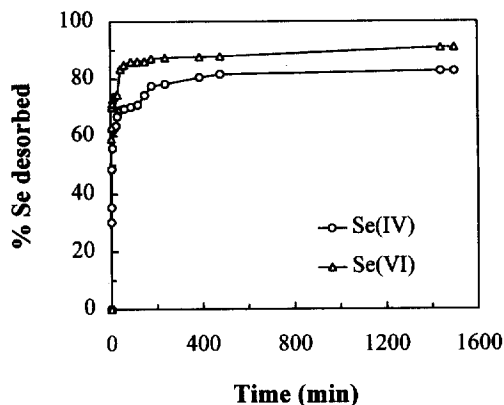


Fig. 4. Desorption kinetics of Se(IV) and Se(VI) on AOCS at pH 12.

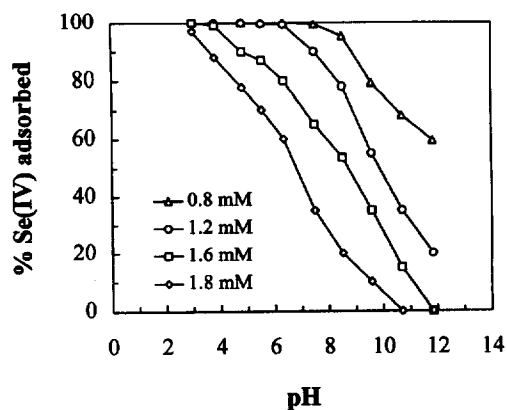


Fig. 5. pH-adsorption edges of Se(IV) on AOCS at various Se(IV) concentrations.

loading, but this phenomenon will be constrained by the concentration of adsorption sites (Hsia *et al.*, 1992). Therefore, the adsorption density on AOCS in concentrated Se(IV) solution will not be greater than that of a more dilute solution. Adsorption of Se(IV) was higher than that of Se(VI) at the same initial concentration at any given pH. That is in good consistence with the results derived from distinguishing various anion affinities based on the first acidity constant (Hayes, 1987; Hayes *et al.*, 1988). Furthermore, removal of Se(IV) remained effective when the system pH was high, suggesting a higher value of $\Delta G_{\text{intr}}^{\circ}$ and that inner-sphere complexation occurs between Se(IV) and Al oxide surfaces.

II Adsorption isotherm. Adsorption parameters for the Langmuir isotherm models are presented in Table 3. The adsorption capacity (Q_m) of Se(IV) and Se(VI) increased as pH decreased, but Q_m of Se(IV) was greater than that of Se(VI) within the pH range of the experiments. At pH 8.50, the adsorption capacity was 0.76 mg of Se(VI)/g AOCS and at pH 7.60 was one-half that at pH 4.90, also revealing that the Se removal capability of AOCS is strongly influenced by the system pH values.

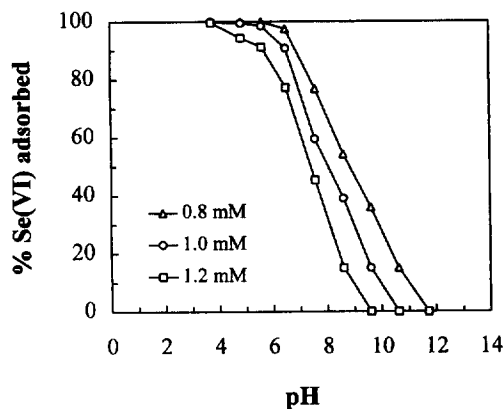


Fig. 6. pH-adsorption edges of Se(VI) on AOCS at various Se(VI) concentrations.

Table 3. Langmuir adsorption isotherm parameters of Se(IV) and Se(VI) sorbed on AOCS^a

pH	Se(IV)			Se(VI)		
	Q_m^b	K^c	r^2^d	Q_m	K	r^2
4.80	1.08	223.60	0.98	—	—	—
4.90	—	—	—	0.92	33.22	0.97
5.70	—	—	—	0.90	38.17	0.98
6.35	0.99	179.50	0.99	—	—	—
6.50	—	—	—	0.75	2.92	0.99
7.48	0.84	7.52	0.99	—	—	—
7.60	—	—	—	0.44	0.24	0.99
8.50	0.76	1.38	0.99	—	—	—

^aLangmuir equation: $Q_e = Q_m K C_e / (1 + K C_e)$.^b Q_m is the adsorption maximum in the Langmuir model (mg Se/g AOCS).^c K is the Langmuir affinity constant.^d r^2 is the determination coefficient of linear regression

III Competition adsorption. Se(IV) and Se(VI) usually coexist in natural water and compete with each other for surface sites on the adsorbent surface. At a Se(VI)/Se(IV) molar ratio of 1 or 3, Se(IV) adsorption efficiency decreased to 70% between pH 3 ~ 8 but was similar to the efficiency of the system containing only Se(IV) within the range of pH 8 ~ 12 (Fig. 7). The pH-adsorption edges of Se(VI) at different Se(IV)/Se(VI) molar ratios are illustrated in Fig. 8. An increase in Se(IV) concentration decreased the adsorption efficiency of Se(VI) and caused the adsorption edges to shift to the left.

It has been demonstrated that, at a ratio higher than 4.5 mmole Al/g SiO₂, Al(OH)₃ completely covers SiO₂ particle surfaces and the pH_{pzc} value of the Al(OH)₃-modified SiO₂ is the same as that of pure Al(OH)₃ (Meng and Letterman, 1993a; 1993b). The critical value can be divided by the BET surface area of SiO₂ (200 m²/g SiO₂) and expressed as 0.023 mmole Al/m² SiO₂. In this study, the BET surface area of quartz sand was 0.20 m²/g sand, obviously lower than powder SiO₂ due to the larger particle size. As a consequence, the sand surface was almost

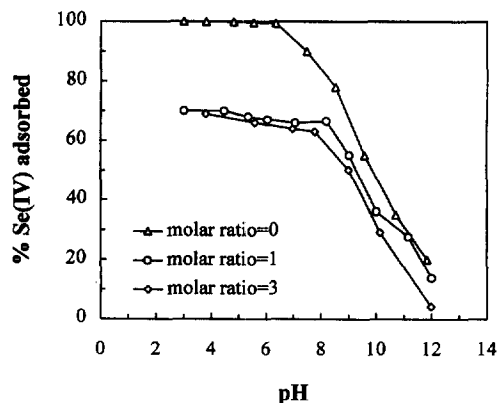


Fig. 7. pH-adsorption edges of Se(IV) on AOCS at various concentrations of coexistence with Se(VI) (Se(IV) = 1.2 mM, Se(VI)/Se(IV) molar ratios = 0, 1, 3).

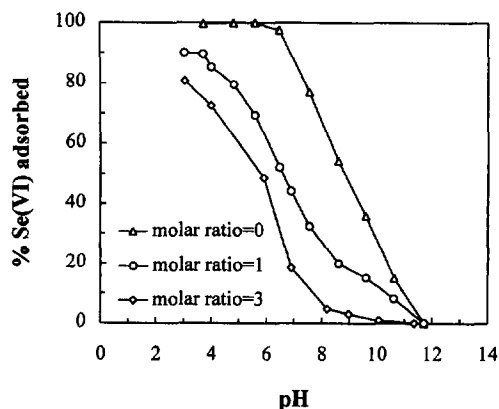
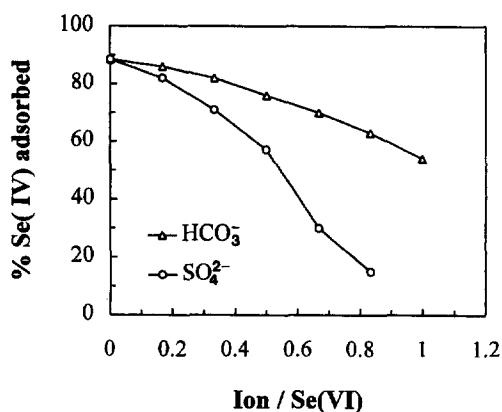


Fig. 8. pH-adsorption edges of Se(VI) on AOCS at various concentrations of coexistence with Se(IV) (Se(VI) = 0.8 mM, Se(IV)/Se(VI) molar ratios = 0, 1, 3).

completely covered with Al oxides and the pH_{pzc} of AOCS was similar to individual amorphous Al oxides (~8.0) (Parks, 1965). Since Se(VI) forms outer-sphere complexes and binds more weakly to AOCS, it can not compete with Se(IV) on negatively-charged AOCS surfaces at $pH > pH_{pzc}$ (Hayes *et al.*, 1988). At system pH ranging from 3 ~ 8 ($< pH_{pzc}$), on the other hand, Se(IV) and Se(VI) compete with each other for available binding sites on the surface of AOCS. However, after the lower energy sites become fully occupied, Se(VI) can no longer compete with Se(IV) for the other surface sites even if the concentration of Se(VI) is increased. Hence, the adsorption edge curves for Se(VI)/Se(IV) molar ratios of 1 and 3 nearly overlap each other.

Sulfate (SO_4^{2-}) and bicarbonate (HCO_3^-) are also common anions in natural aqueous systems, and their existence substantially reduce the Se removal efficiency of AOCS. Differences in the reduction of Se adsorption in the presence of SO_4^{2-} and HCO_3^- can be related to their different complex formation characteristics with metal oxide surfaces. The evi-

Fig. 9. Adsorption of Se(IV) on AOCS at various concentrations of HCO_3^- and SO_4^{2-} .

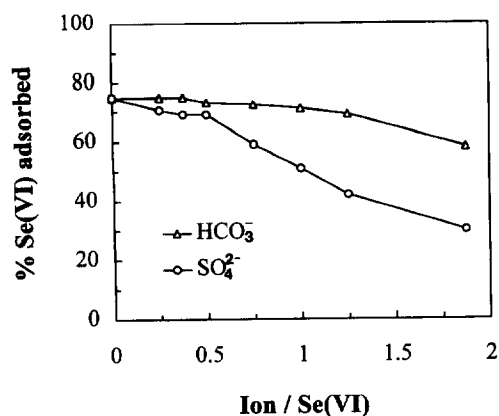


Fig. 10. Adsorption of Se(VI) on AOCS at various concentrations of HCO_3^- and SO_4^{2-} .

dence derived from infrared spectroscopic studies has shown that an adsorbed SO_4^{2-} ion can replace two A-type hydroxyl groups singly coordinated to two metal ions (Parfitt and Smart, 1978; Rajan, 1978). HCO_3^- does not form in a binuclear mode by bonding two oxygens of the anion into the positions previously occupied by two hydroxyls on the oxide surface as SO_4^{2-} does (Serna et al., 1977; White and Hem, 1975). Adsorption of Se(IV) and Se(VI) on AOCS in the presence of varying concentrations of foreign anions is displayed in Figs 9–10. The sequence of competition with respect to both Se(IV) and Se(VI) adsorption is in the order of $\text{SO}_4^{2-} > \text{HCO}_3^-$.

CONCLUSIONS

Quartz sand coated at 70°C using 1 M AlCl_3 solution at $\text{pH}_{(\text{coating})}$ 5.98 for 2 d is recommended as an efficient adsorbent for advanced water treatment. The results reveal that the adsorption rate of Se(IV) increases more rapidly than that of Se(VI) in the initial period, and both of them reach metastable equilibrium within 60 mins. The adsorption for Se(IV) onto AOCS surfaces is higher than that for Se(VI) under the same system pH (3 ~ 12). The Langmuir monolayer adsorption capacity also indicates that the removal of Se(IV) is more effective than that of Se(VI). Since Se(VI) adsorption involves the formation of outer-sphere complexes, it can not affect Se(IV) adsorption at higher pH. Whether the Se(VI)/Se(IV) molar ratio is 1 or 3, the Se(IV) adsorption curve shifts in accordance. However, Se(VI) adsorption is greatly influenced by the amount of Se(IV) that coexists in the system at all pH. The competition adsorption of sulfate (SO_4^{2-}) with respect to Se(IV) and Se(VI) is more evident than that of bicarbonate (HCO_3^-).

Acknowledgements—We thank the National Science Council of Taiwan, Republic of China, NSC # 83-04110-E-002-082 for financial support.

REFERENCES

- Alloway B. J. (1995) *Heavy Metals in Soils*. Blackie Academic & Professional, an Imprint of Chapman & Hall, USA.
- Bailey R. P., Bennett T. and Benjamin M. M. (1992) Sorption onto and recovery of Cr(VI) using iron-oxide-coated sand. *Wat. Sci. Technol.* **26**, 1239–1244.
- Balistreri L. S. and Chao T. T. (1987) Selenium adsorption by goethite. *Soil Sci. Soc. Am. J.* **51**, 1145–1151.
- Blaylock M. J. and James B. R. (1993) Selenite and selenate quantification by hydride generation-atomic absorption spectrometry, ion chromatography, and colorimetry. *J. Environ. Qual.* **22**, 851–857.
- Bleam W. F. and McBride M. B. (1985) Cluster formation versus isolated-site adsorption. A study of Mn(II) and Mg(II) adsorption on boehmite and goethite. *J. Colloid Interface Sci.* **103**, 124–132.
- Davis J. A. and Leckie J. O. (1980) Surface ionization and complexation at the oxide/water interface. III. Adsorption of anions. *J. Colloid Interface Sci.* **74**, 32–43.
- DeBoer J. H., Fortuin J. M. H., Lippens B. C. and Meijers W. H. (1963) Study of the nature of surfaces with polar molecules. II. The adsorption of water on aluminas. *J. Catal.* **2**, 1–7.
- Dzombak D. A. and Morel F. M. M. (1990) *Surface Complexation Modeling*. John Wiley and Sons, New York.
- Edwards M. and Benjamin M. M. (1989) Adsorption filtration using coated sand: a new approach for treatment of metal-bearing wastes. *J. Wat. Pollut. Control Fed.* **61**, 1523–1533.
- Hayes K. F. (1987) *Equilibrium, Spectroscopic and Kinetic Studies of Ion Adsorption at the Iron oxide/aqueous interface*. Ph.D. Dissertation, Stanford University, Stanford, CA.
- Hayes K. F., Papelis C. and Leckie J. O. (1988) Modelling ionic strength effects on anion adsorption at hydrous oxide/solution interfaces. *J. Colloid and Interface Sci.* **125**, 717–726.
- Hsia T. H., Lo S. L., Lin C. F. and Lee D. Y. (1992) Interaction of Cr(VI) with amorphous iron oxide adsorption density and surface charge. *Wat. Sci. Technol.* **26**, 181–188.
- Jacobs L. W. (1989) *Selenium in Agriculture and the Environment*. American Society of Agronomy, Inc., Madison, WI.
- Lai C. H., Lo S. L. and Lin C. F. (1994) Evaluating an iron-coated sand for removing copper from water. *Wat. Sci. Technol.* **30**, 175–182.
- Lakin H. W. (1973) Selenium in our environment. *Adv. Chem. Series* **123**, 96–111.
- Lo S. L., Jeng H. T., Lin C. F. and Lee D. Y. (1994) Adsorption of heavy metals by the iron-coated filter medium. *J. Chinese Inst. of Civil and Hydraulic Eng.* **6**, 101–110.
- Mason B. (1960) *Principle of Geochemistry*. John Wiley and Sons, New York.
- Meng X. and Letterman R. D. (1993a) Effect of component oxide interaction on the adsorption properties of mixed oxides. *Environ. Sci. Technol.* **27**, 970–975.
- Meng X. and Letterman R. D. (1993b) Modeling ion adsorption on aluminum hydroxide modified silica. *Environ. Sci. Technol.* **27**, 1924–1929.
- Meng X. and Letterman R. D. (1996) Modeling cadmium and sulfate adsorption by $\text{Fe}(\text{OH})_3/\text{SiO}_2$ mixed oxides. *Wat. Res.* **30**, 2148–2154.
- Neal R. H., Sposito G., Holtzclaw K. M. and Traina S. J. (1987) Selenite adsorption on alluvial soils: I. soil composition and pH effects; II. solution composition effects. *Soil Sci. Soc. Am. J.* **51**, 1161–1169.

- Parfitt R. L. and Smart R. S. (1978) The mechanisms of sulfate adsorption on iron oxides. *Soil Sci. Soc. Am. J.* **42**, 48–50.
- Parks G. A. (1965) The isoelectric points of solid oxides, solid hydroxides, and aqueous hydroxy-complex systems. *Chem. Rev.* **65**, 177–198.
- Rajan S. S. S. (1978) Sulfate adsorbed on hydrous alumina, ligands, displaced and changes in surface charge. *Soil Sci. Soc. Am. J.* **42**, 39–44.
- Scott M. J. and Morgan J. J. (1996) Reactions at oxide surfaces. II. Oxidation of Se(IV) by synthetic birnessite. *Environ. Sci. Technol.* **30**, 1990–1996.
- Serna C. J., White J. L. and Hem S. L. (1977) Anion-aluminum hydroxide gel interactions. *Soil Sci. Soc. Am. J.* **41**, 1009–1013.
- Sposito G. (1983) On the surface complexation model of the oxide-aqueous solution interface. *J. Colloid Interface Sci.* **91**, 329–340.
- Sposito G. (1984) *The Surface Chemistry of Soils*. Oxford University Press, New York.
- Stahl R. S. and James B. R. (1991) Zinc sorption by iron-oxide-coated sand as a function of pH. *Soil Sci. Soc. Am. J.* **55**, 1287–1290.
- White J. L. and Hem S. L. (1975) Role of carbonate in aluminum hydroxide gel established by Raman and IR analyses. *J. Pharm. Sci.* **64**, 468–469.
- Zhang P. and Sparks D. L. (1990) Kinetics of selenate and selenite adsorption/desorption at the goethite/water interface. *Environ. Sci. Technol.* **24**, 1848–1856.